Available online at www.sciencedirect.com
SCIENCE DIRECT®
Journal of Nuclear Materials 321 (2003) 170–176
journal of nuclear materials
www.elsevier.com/locate/jnucmat

Compatibility studies in the $Li_{17}Pb_{83}$–SiC, Be–SiC and Be–Mo systems

H. Kleykamp *

Forschungszentrum Karlsruhe, Institut für Materialforschung I, Postfach 3640, 76021 Karlsruhe, Germany

Received 13 February 2003; accepted 17 April 2003

Abstract

The compatibility of $Li_{17}Pb_{83}$ with SiC between 600 and 1000 °C, of Be with SiC between 700 and 900 °C and of Be with Mo between 800 and 900 °C was studied isothermally in capsule experiments. About 0.017, 0.035 and <0.05 mass% Si were observed in the $Li_{17}Pb_{83}$ melt annealed at 600, 800 and 1000 °C, resp. The reaction between Be and SiC is unidirectional and rate-determined by Be diffusion through the product phases Si and Be_2C with the chemical diffusion coefficient $\widetilde{D}_{Be} = 3.0 \cdot 10^{-5} \exp(-224000/RT)$ m^2/s, 1000–1350 K. The lattice parameter of fcc Be_2C was found to $a = 434.9$ pm. The reaction between Be and Mo is unidirectional and rate-determined by Be diffusion through the product phases $Be_{12}Mo$ and Be_2Mo. The compound $BeMo_3$ was observed only during the 800 °C heat treatment.

1. Introduction

New first-wall structural materials have been proposed and are being investigated as possible candidates for advanced concepts within the blanket activities of the European fusion reactor programme. Among them are SiC fibre-reinforced SiC fabrics (f-SiC/SiC) in their hermetically sealed form. The material is characterised by very low neutron activation and a reasonable stability. The compatibility is uncertain with beryllium and solid breeder ceramics, e.g. Li_4SiO_4, Li_2ZrO_3 and Li_2TiO_3, within the advanced helium-cooled pebble bed blanket concept [1] and with liquid lithium containing materials of the self-cooled liquid Pb–17Li blankets, e.g. in the ARIES-AT concept [2]. Further, the compatibility of the neutron multiplier beryllium with the capsule material molybdenum is of interest in regard of the direct Mo tube heating up to 1000 °C in the radiation field of a high-flux reactor.

Three series of compatibility tests were performed to elucidate these subjects: (1) Liquid $Li_{17}Pb_{83}$ with α-SiC crucibles between 600 and 1000 °C. (2) Stacks of polished β-SiC/Be/β-SiC disks annealed in Mo capsules between 700 and 900 °C. (3) Stacks of polished Mo/Be/Ta disks annealed in Mo capsules between 800 and 900 °C.

2. Literature survey

2.1. $Li_{17}Pb_{83}$–SiC compatibility

Compatibility tests were conducted between α-SiC tube sections and liquid $Li_{17}Pb_{83}$ in welded austenitic steel capsules (No. 1.4948) between 300 and 700 °C for 100 h in each case. A pronounced chemical attack of SiC by $Li_{17}Pb_{83}$ was observed which increased with increasing temperature up to 500 °C, however, quantitative results were not given. The reaction behaviour at 600 and 700 °C was unclear. Further experiments were made at 600 °C with zirconium additions in order to get the oxygen contaminations from the melt. The SiC tube section was completely corroded. An interpretation of this result was not given [3]. The addition of Zr initiates

* Tel.: +49-7247 822888; fax: +49-7247 824567.
E-mail address: heiko.kleykamp@imf.fzk.de (H. Kleykamp).

0022-3115/$ - see front matter © 2003 Elsevier B.V. All rights reserved.
doi:10.1016/S0022-3115(03)00247-2

the formation of the compound $PbZr_2C$ [4] and dissolution of SiC in the $Li_{17}Pb_{83}$ melt according to the reaction

$$SiC + Li_xPb + 2Zr = PbZr_2C + Li_xSi \quad (1)$$

Possibly, the austentic steel components M will have a similar effect initiated by the formation of ternary Pb–M–C compounds.

Other compatibility tests were conducted between SiC (fibre-reinforced and monolithic) and liquid $Li_{17}Pb_{83}$ in welded molybdenum containers at 800 °C for 1500 h. No corrosion attack was observed [5]. The reason might be the inability of a ternary Pb–Mo–C phase formation. SiC–$Li_{17}Pb_{83}$ compatibility studies in molybdenum crucibles have shown no corrosion effects at 300 and 500 °C after 667 h [6]. Further compatibility studies of $Li_{17}Pb_{83}$ with SiC mounted in a TZM holder at 800 °C for 3000 h indicated no reaction. However, about 0.0008 mass% Si was found in $Li_{17}Pb_{83}$ [7]. This result could be substantiated with the precipitation of $PbZr_2C$ in the liquid according to Eq. (1).

2.2. Beryllium–SiC compatibility

Early compatibility studies between α-SiC single crystals and Be at 1050 and 1150 °C were reported by Matyushenko et al. [8]. More recent investigations were carried out between β-SiC tiles and Be disks within closed Mo capsules at 900 °C up to 70 days. The measured layer thickness, the X-ray microanalysis (XMA) of the reaction products Be_2C and Si between SiC and Be and the unidirectional material transport of Be through the reaction zone gave a tentative value of the chemical diffusion coefficient $\widetilde{D}_{Be}$ of Be in the reaction zone, $\widetilde{D}_{Be} = 2.6 \times 10^{-15}$ m^2/s at 900 °C [9] according to the reaction

$$2Be + SiC = Be_2C + Si \quad (2)$$

2.3. Beryllium–molybdenum compatibility

Early diffusion studies of Be vapour which was deposited on a Mo surface have shown by X-ray diffraction after annealing between 900 and 1250 °C that the main product phase has the composition $Be_{22}Mo$. A preferential Be diffusion occurred through the formed alloy [10]. Mo fibres were embedded in Be powder and were hot-pressed between 900 and 1100 °C with no hold time at these temperatures. Be–Mo reactions were observed at 1000 °C and above. The cylindrical reaction product layers were analysed by XMA resulting in the compositions $Be_{12}Mo$ and Be_2Mo. There was no evidence of the formation of a $Be_{22}Mo$ or $BeMo_3$ phase [11]. The solid-state reaction between Mo and $Be_{13}Zr$ or $Be_{13}Y$ between 900 and 1500 °C resulted in the formation of Be_2Mo in the contact zone. No other Mo beryllides were observed [12].

3. Experimental

3.1. $Li_{17}Pb_{83}$–SiC compatibility studies

The Pb–17at.% Li ingots were delivered by Métaux Spećiaux S.A., Paris. The oxygen impurity content was below the detection limit of 2 μg/g. The single-phase hexagonal α-SiC crucibles with 98% theor. density and 0.1% B and >0.1% Al sintering aids were obtained from Elektroschmelzwerk Kempten, Kempten. The dimensions were, height 18 mm, outer diameter 18 mm, wall thickness 3 mm. The crucible of each experiment was made complete in an argon-filled glove box with about 6 mm high Li–Pb, was set into an open Al_2O_3 crucible and this was set into an austentic steel crucible (No. 1.4571, X10 CrNiMoTi 1810) for the 600 and 800 °C experiments and into a scale-resistant nickel base alloy crucible (No. 2.4851, X10 NiCr23Fe) for the 1000 °C experiment. The Al_2O_3 crucible was necessary to avoid the SiC incompatibility with the alloys resulting in silicides formation. The steel and nickel alloy crucibles were closed with lids of the same materials by electron beam welding under high vacuum. The static isothermal heat treatments of the electron beam welded containers were carried out under air in a temperature controlled furnace for 672 h in each experiment. Subsequently, the SiC crucibles were cut and polished by diamond emery down to 0.3 μm perpendicular to the cylinder axis. X-ray microanalysis (XMA) of Si (Kα line) and Pb (Mα line) was done by WDX, that of C was not possible due to the interference of the C Kα line with the Pb N–N transitions in the wavelength region 4.2–4.5 nm. Step scans were made between the surface of the cylindrical ingots and their central axis along about 6 mm distance. The measured Si intensities were converted to concentrations by the ZAF correction method. The classical integral chemical analysis of C in the Pb–17at.% Li melt was carried out by combustion of C in an induction-heated furnace to CO_2 and of Si by the ICP-OES method.

3.2. Beryllium–SiC compatibility studies

The materials used as well as the procedure for the isothermal compatibility studies, the metallography and the quantitative XMA of Be, C, O and Si were reported in [9]. More details on the Be analysis were given in [13]. Further investigations were made on the reaction products by X-ray diffractometry using a Seyfert XRD-3000 diffractometer in the 2θ range between 21° and 122°, Cu Kα radiation with $\lambda = 154.178$ pm, a graphite

monochromator and calibration with the internal β-SiC standard.

3.3. Beryllium–molybdenum compatibility studies

Beryllium disks of 8 mm diameter and 0.5 mm thickness were manufactured by W.C. Heraeus, Hanau. The chemical analysis of the supplier gave >99.83% Be purity. Molybdenum disks of the same diameter and about 2 mm thickness were cut from Mo plates supplied by Climax Comp., USA; purity > 99.7% Mo. The isothermal compatibility studies were carried out using stacks of Mo–Be–Ta disks in screwed Mo capsules at (800 ± 1) and (900 ± 1) °C for 1000 h in each case. The metallography of the cuts and the quantitative X-ray microanalysis of Be and Mo were reported in [9,13].

4. Results

4.1. $Li_{17}Pb_{83}$–SiC compatibility studies

The 600 °C experiment resulted in a cross-section averaged Si concentration in the solidified Li–Pb melt of 0.017 mass% Si, which increased to 0.08 mass% Si in the outer surface region (Fig. 1). The amount of 0.017 mass% Si corresponds to 0.0073 mass% C as SiC dissolution is assumed yielding a $c_{SiC} = 0.000243$ mass fraction in Li–Pb. Geometrical considerations result in an inner SiC crucible wall eroded layer of $d_{SiC} = 1.7$ μm. An ingot averaged Si concentration of 0.035 mass% Si and a surface near concentration increase up to 0.3 mass% Si were obtained at 800 °C under the same experimental and analytical conditions (Fig. 2). A SiC wall

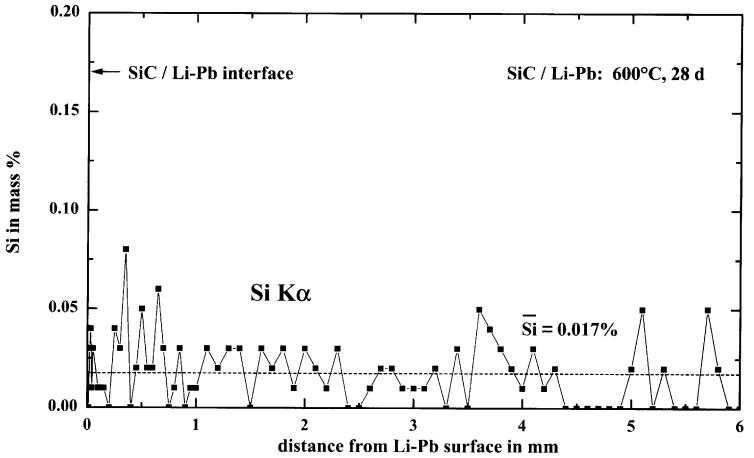

Fig. 1. Si concentration at 600 °C in the $Li_{17}Pb_{83}$ melt contained in a SiC crucible vs. distance from the SiC/$Li_{17}Pb_{83}$ interface.

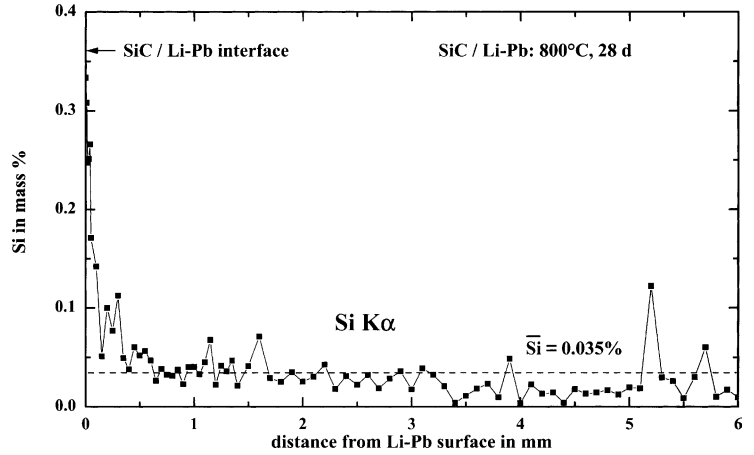

Fig. 2. Si concentration at 800 °C in the $Li_{17}Pb_{83}$ melt contained in a SiC crucible vs. distance from the SiC/$Li_{17}Pb_{83}$ interface.

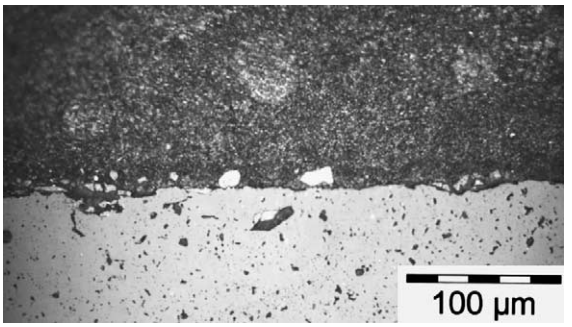

Fig. 3. Light-optical microstructure of the inner SiC crucible surface region in contact with the $Li_{17}Pb_{83}$ melt after 1000 °C/672 h.

erosion of $d_{SiC} = 3.6$ μm is estimated at this temperature. The evaluation of the 1000 °C experiment is more difficult. The microstructure of the inner SiC crucible surface region has shown a frayed and roughened morphology (Fig. 3). Small SiC or eventually Si–Pb–C grains with a diameter between <1 and 5 μm were observed in the solidified Li–Pb melt. Therefore, a quantitative X-ray microanalysis was not possible within the solidified melt. However, a classical chemical analysis of the ingot was carried out which gave averaged values < 0.05 mass% Si and (0.0240 ± 0.0005) mass% C.

4.2. Beryllium–SiC compatibility studies

Isotherms of the reaction between Be and β-SiC disks were obtained at 700, 800, 850 and 900 °C up to 104 days. X-ray microanalysis and X-ray diffraction revealed that the reaction layer between the starting materials is two-phase and is composed of interconnected Be_2C and Si. A gap was observed between the reaction products and the Be disk which is an indication of unidirectional Be diffusion into the SiC phase.

A very thin reaction layer between Be an β-SiC was observed at the lowest investigated 700 °C isotherm after long reaction time $t = 70$ days which resulted in a thickness $x = (10 \pm 4)$ μm (see Fig. 4). The 800, 850 and 900 °C isotherms were fitted to a parabolic curve due to a diffusion-controlled reaction $x^2 = 2 \cdot \widetilde{D}_{Be} \cdot t$ where $\widetilde{D}_{Be}$ is the chemical diffusion coefficient of Be in the reaction products. The error bars in Fig. 4 represent the variations of the thickness of the reaction products in different positions. The diffusion coefficients are compiled in Table 1. The slope of the graphical representation of $\log \widetilde{D}_{Be}$ as a function of the reciprocal temperature $1/T$ results in the energy of activation $q = 224$ kJ/mol of the rate-determined step of the reaction $2\,Be + SiC = Be_2C + Si$ and the temperature dependence of the chemical diffusion coefficient

$$\widetilde{D}_{Be} = 3.0 \cdot 10^{-5} \cdot \exp(-q/RT)\ m^2/s \quad (3)$$

in the temperature range 1000–1350 K (see Fig. 5). Eq. (3) can be used to calculate, by extrapolation of the temperature, the Be_2C–Si layer formation, e.g. at 600 °C = 873 K which is the maximum operation temperature of Be in a SiC container of the fusion reactor blanket concept. The layer thickness is $x = 2.5$ μm after 30 days and $x = 7.8$ μm after 300 days operation time.

Four peaks of Be_2C were clearly identified in the X-ray diffraction diagram (see Table 2) which results in the lattice parameter $a = (434.9 \pm 0.2)$ pm of fcc CaF_2-type Be_2C.

The chemical shift of the Be Kα line is a further indication of the nature of the Be containing phases which can be detected if the spectral resolution of the relevant analytical instrument is adequate. The wavelength of the emitted Be Kα line was measured by XMA what

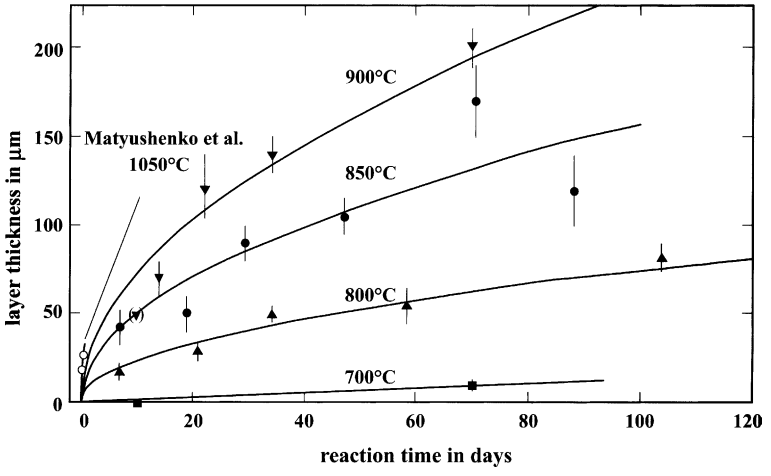

Fig. 4. Isotherms of the Be_2C–Si layer formation by reaction of the Be–SiC pellet couple.

Table 1
Chemical diffusion coefficient $\widetilde{D}_{Be}$ of Be in the Be_2C–Si reaction product layer

$\widetilde{D}_{Be}$ in m^2/s	T in K	Ref.
$(3.2 \pm 0.8) \times 10^{-16}$	1073	This work
$(1.4 \pm 0.6) \times 10^{-15}$	1123	This work
$(3.1 \pm 0.7) \times 10^{-15}$	1173	This work
$(4.1 \pm 0.6) \times 10^{-14}$	1323	[8]

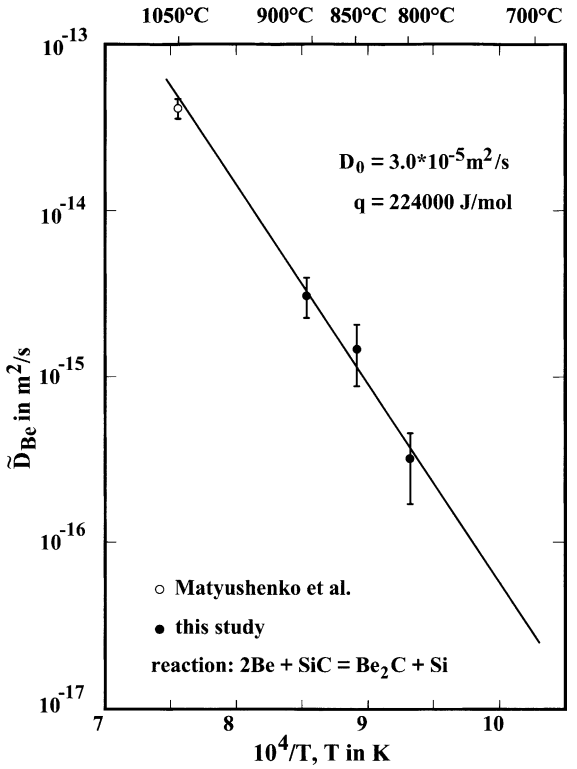

Fig. 5. Chemical diffusion coefficient $\widetilde{D}_{Be}$ of Be in the Be_2C–Si reaction zone as a function of the inverse temperature.

Table 2
X-ray diffraction diagram of Be_2C, Cu Kα radiation, $\lambda = 154.178$ pm

2θ in °	hkl	a in pm
35.75	1 1 1	435.0
60.15	2 2 0	435.1
72.04	3 1 1	434.8
120.6	4 2 2	434.8

amounts to $\lambda = 11.35$ nm in Be metal [13], $\lambda = 11.48$ nm in Be_2C [14], $\lambda = 11.53$ nm in Be_3N_2 (a Be disk was nitrided in nitrogen at 900 °C, unpublished), and $\lambda = 11.65$ nm in BeO [13].

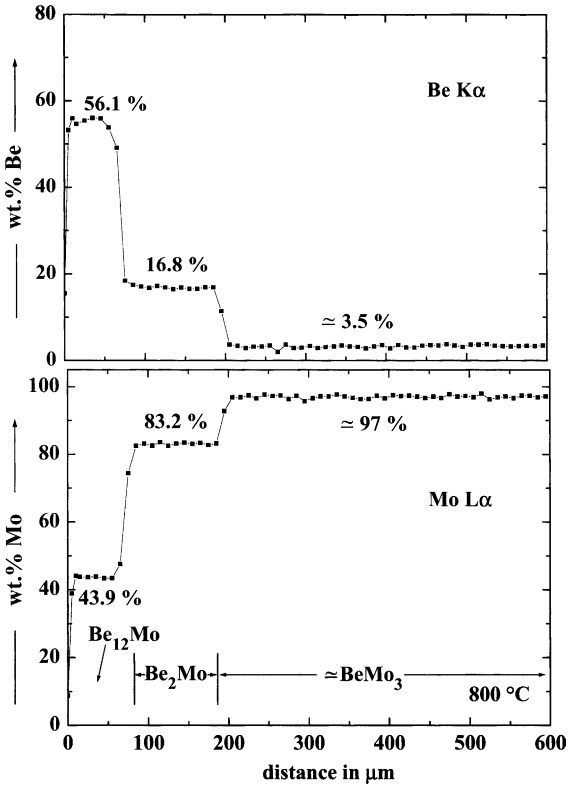

Fig. 6. X-ray microanalysis profiles of Be and Mo in the $Be_{12}Mo$, Be_2Mo and $BeMo_3$ layers formed between Be an Mo at 800 °C/1000 h. The Be disk is separated from the reaction products by a small gap.

4.3. Beryllium–molybdenum compatibility studies

Both the metallographic cuts of the 800 and 900 °C heat treatments have shown a 40–70 μm thick gap between the thinned Be disk and the Mo containing phases. Fig. 6 illustrates the sequence of the observed Be–Mo phases of the 800 °C heat treatment: $Be_{12}Mo$ (80 μm), Be_2Mo (100 μm) and $BeMo_3$ with a thickness larger than 500 μm (not completely shown in Fig. 5). The intermetallic compound $Be_{22}Mo$ was not observed. Fig. 7 explains the sequence of the observed Be–Mo phases of the 900 °C heat treatment: $Be_{12}Mo$ (200 μm) and Be_2Mo (170 μm). In other positions than that of Fig. 7, the $Be_{12}Mo$ layer thickness was reduced down to 13 μm (Fig. 8). The intermetallic compounds $Be_{22}Mo$ and $BeMo_3$ were not observed. The reactions are unidirectional by Be diffusion through the reaction products.

5. Discussion

The analysis of Si in $Li_{17}Pb_{83}$ was carried out in this work by the established quantitative XMA method. The

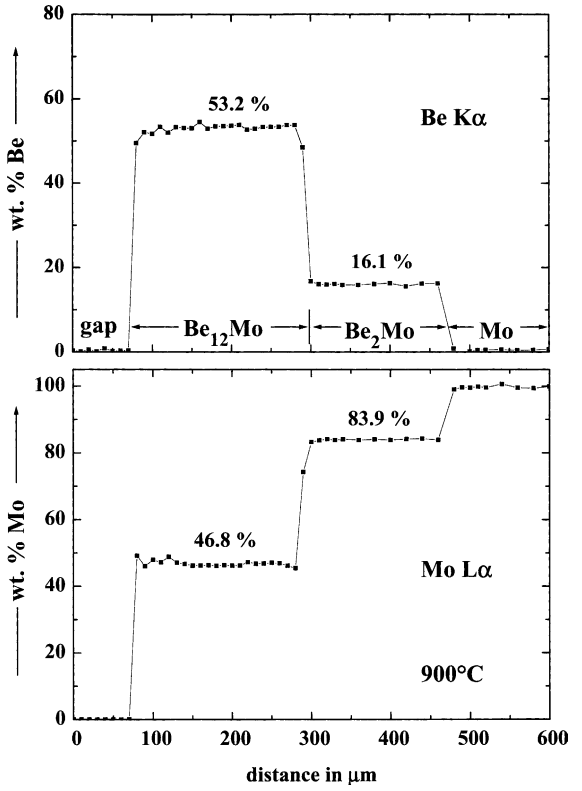

Fig. 7. X-ray microanalysis profiles of Be and Mo in the $Be_{12}Mo$ and Be_2Mo layers formed between Be and Mo at 900 °C/1000 h. The Be disk is separated from the reaction products by a small gap.

detection limit is <0.01 mass% Si. The simultaneous dissolution of Si and C by inside wall erosion of the SiC crucible in the 600 and 800 °C experiments remains unclear. However, a C enrichment on the inside wall could not be detected. The erosion at 1000 °C is connected with the pull-out of small SiC grains from the inner crucible surface. The formation of a ternary Pb–Si–C phase in $Li_{17}Pb_{83}$ cannot be excluded. The contradictory results of the Si and C analysis in $Li_{17}Pb_{83}$ carried out by other methods [3,5–7] cannot be fully duplicated by the present author. A long-time use of SiC in contact with $Li_{17}Pb_{83}$ at 1000 °C is questionable.

The chemical diffusion coefficient $\tilde{D}_{Be}$ of Be in the Be_2C–Si product phases between 973 and 1173 K reported in this work agrees well with the result of Mutyushenko et al. measured at 1323 K [8] (see Fig. 4). The rate-determined step of the Be bulk diffusion is caused by one of the product phases, probably in Be_2C. The self-diffusion of Be in polycrystalline material was reported in [15] to

$$D_{Be} = 0.36 \cdot 10^{-4} \cdot \exp(-160\,800/RT)\ \mathrm{m^2/s} \quad (4)$$

between 923 and 1473 K, q in J/mol. The interstitial impurity diffusion of Be in p-type α-SiC was reported in [16] to

$$D_{Be}^{SiC} = 10^{-8} \cdot \exp(-145\,000/RT)\ \mathrm{m^2/s} \quad (5)$$

approximately between 1200 and 2000 K, q in J/mol. The impurity diffusion of Be in Si can be derived with reservation from ion implantation experiments which results in [17,18]

$$D_{Be}^{Si} = 1 \cdot 10^{-2} \exp(-193\,000/RT)\ \mathrm{m^2/s} \quad (6)$$

between 1050 and 1300 K, q in J/mol.

The following conclusions can be drawn by comparison of the diffusion coefficients given in Eqs. (3)–(6). The self-diffusion coefficient of Be at 1100 K is of the order of 10^{-12} m^2/s, whereas the impurity diffusion coefficient of Be in Si and in SiC as well as the chemical diffusion coefficient in the Si–Be_2C reaction product are of the order of 10^{-15} m^2/s. The isothermal kinetics has proven a $t^{1/2}$ time law. These results reveal that the unidirectional Be diffusion in the product phases is the time-determining step.

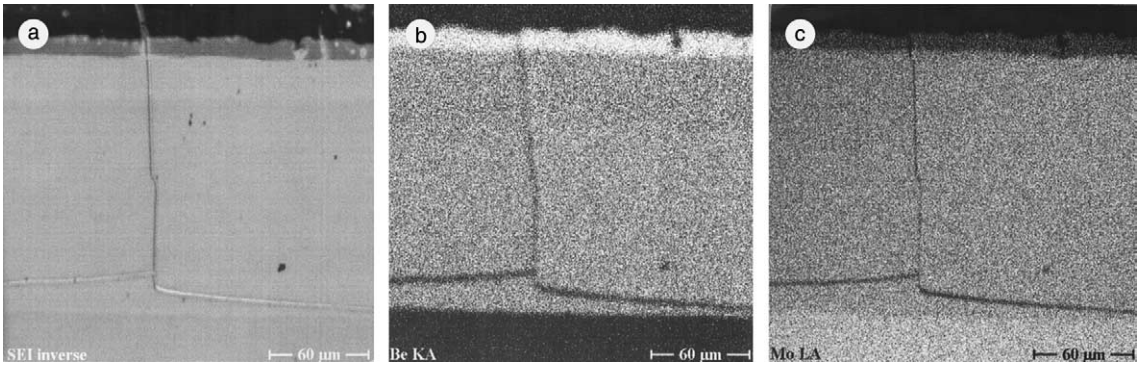

Fig. 8. Electron-optical microstructure of the products of the Be–Mo reaction after 900 °C/1000 h: SEI, secondary electron image; Be, beryllium Kα distribution; Mo, molybdenum Lα distribution. Layer sequence: gap (top), 13 μm $Be_{12}Mo$, 140 μm Be_2Mo, Mo (bottom).

The Be–Mo compatibility tests are screening experiments within the reaction kinetics programme of Be with structure materials. The incompatibility between these two metals at 800 and 900 °C is dramatic. The extreme reactivity at these temperatures indicates by extrapolation to 500–600 °C that the structural material Mo should be incompatible with the neutron multiplier Be at the maximum operation temperatures of a fusion reactor blanket.

Four intermediate phases exist in the Be–Mo system [19]: $Be_{22}Mo$, peritectic formation at 1300 °C; $Be_{12}Mo$, congruent melting at 1690 °C, Be_2Mo, congruent melting at 2027 °C; $BeMo_3$, peritectoidal formation at 900 °C. The existence of $Be_{22}Mo$ was not observed between 800 and 900 °C and should be reconsidered; the peritectoidal formation of $BeMo_3$ occurred only below 900 °C. The experimental results deserve a comparison with the actual phase diagram of the Be–Mo system [19].

Acknowledgements

The author acknowledges the assistance of Mr O. Wedemeyer for the capsule heat treatment experiments, Mr R. Rolli for the metallography and the X-ray diffraction of the samples, Dr C. Adelhelm for the chemical analysis and Mr H.D. Gottschalg for the X-ray microanalysis work.

References

[1] L.V. Boccaccini, U. Fischer, S. Gordeev, S. Malang, Fusion Eng. Des. 49&50 (2000) 491.
[2] R.H. Jones, L.L. Snead, A. Kohyama, P. Fenici, Fusion Eng. Des. 41 (1998) 15.
[3] H. Runge, Internationale Atomreaktorbau GmbH, unpublished report, 1984.
[4] W. Jeitschko, H. Nowotny, H. Benesovsky, J. Less-Common Met. 7 (1964) 133.
[5] V. Coen, H. Kolbe, L. Orecchia, M. Della Rossa, in: R.J. Fordham (Ed.), High Temp. Corrosion of Techn. Ceram., Elsevier, 1990;
P. Fenici, H.W. Scholz, J. Nucl. Mater. 212–215 (1994) 60.
[6] T. Terai, T. Yoneoka, S. Tanaka, in: Int. Town Meeting on SiC/SiC Design and Mater. Issues for Fusion Systems, ORNL, unpublished report, 2000.
[7] F. Barbier, Ph. Deloffre, A. Terlain, J. Nucl. Mater. 307–311 (2002) 1351.
[8] N.N. Matyushenko, A.A. Rozen, N.S. Pugachev, Sov. Powder Metall. Met. Ceram. 5 (1966) 310.
[9] H. Kleykamp, J. Nucl. Mater. 283–287 (2000) 1385.
[10] N.N. Matyushenko, Russ. Metall. 2 (1964) 107.
[11] C.R. Watts, Trans. Met. Soc. AIME 245 (1969) 329.
[12] A.S. Panov, M.M. Rysina, Russ. Metall. 1 (1970) 133; 5 (1977) 202.
[13] H. Kleykamp, J. Anal. Atomic Spectrom. 14 (1999) 377.
[14] H. Kleykamp, Röntgenmikroanalyse in Beryllium kommerzieller Qualitäten zum Löslichkeits- und Ausscheidungsverhalten von Verunreinigungen, 11. Tagung Festkörperanalytik, Chemnitz, 25–28 Juni 2001, Tagungsbericht, S. 116.
[15] L.V. Pavlinov, G.V. Grigorev, V.G. Sevastianov, Fiz. Met. Metalloved. 25 (1968) 565.
[16] Yu.A. Vodakov, E.N. Mokhov, V.G. Oding, Inorg. Mater. 19 (1983) 97.
[17] H. Tomokage, M. Hagiwara, K. Hashimoto, Mem. Fac. Eng. Kyushu Univ. 42 (1982) 89.
[18] V. Hadjicontis, C.A. Londos, K. Eftaxias, Phys. Stat. Sol. (a) 105 (1988) K87.
[19] H. Okamoto, Phase Diagrams for Binary Alloys, ASM, Materials Park, 2000.